

# Dynamics of calcium regulation of chloride currents in *Xenopus* oocytes

AKINORI KURUMA AND H. CRISS HARTZELL

Department of Cell Biology, Emory University School of Medicine, Atlanta, Georgia 30322-3030

**Kuruma, Akinori, and H. Criss Hartzell.** Dynamics of calcium regulation of chloride currents in *Xenopus* oocytes. *Am. J. Physiol.* 276 (*Cell Physiol.* 45): C161–C175, 1999.—Ca-activated Cl currents are widely expressed in many cell types and play diverse and important physiological roles. The *Xenopus* oocyte is a good model system for studying the regulation of these currents. We previously showed that inositol 1,4,5-trisphosphate (IP<sub>3</sub>) injection into *Xenopus* oocytes rapidly elicits a noninactivating outward Cl current ( $I_{Cl-S}$ ) followed several minutes later by the development of slow inward ( $I_{Cl2}$ ) and transient outward ( $I_{Cl-T}$ ) Cl currents. In this paper, we investigate whether these three currents are mediated by the same or different Cl channels. Outward Cl currents were more sensitive to Ca than inward Cl currents, as shown by injection of different amounts of Ca or by Ca influx through a heterologously expressed ligand-gated Ca channel, the ionotropic glutamate receptor iGluR3. These data could be explained by two channels with different Ca affinities or one channel with a higher Ca affinity at depolarized potentials. To distinguish between these possibilities, we determined the anion selectivity of the three currents. The anion selectivity sequences for the three currents were the same (I > Br > Cl), but  $I_{Cl-S}$  had an I-to-Cl permeability ratio more than twofold smaller than the other two currents. The different anion selectivities and instantaneous current-voltage relationships were consistent with at least two different channels mediating these currents. However, after consideration of possible errors, the hypothesis that a single type of Cl channel underlies the complex waveforms of the three different macroscopic Ca-activated Cl currents in *Xenopus* oocytes remains a viable alternative.

inositol trisphosphate; glutamate receptor; voltage clamp; A-23187; store-operated calcium entry

INCREASES IN CYTOSOLIC Ca can occur by Ca influx from the extracellular space or by release of Ca from subcellular compartments (3, 40). For example, many G protein- and tyrosine kinase-associated receptors stimulate phospholipase C and the production of inositol 1,4,5-trisphosphate (IP<sub>3</sub>), resulting in a transient release of Ca from endoplasmic reticulum (ER) stores and then a long-lasting influx of extracellular Ca. This Ca influx, which is stimulated by decreases in the Ca content of internal stores, has been termed store-operated Ca entry (SOCE), formerly known as capacitative Ca entry (41, 42).

*Xenopus* oocytes have been used extensively as a model system for studying Ca signaling and have provided valuable information about spatial and temporal aspects of Ca signals and the mechanisms of

regulation of SOCE. *Xenopus* oocytes are well suited for studies on Ca signaling, because they are easily voltage clamped with two microelectrodes (10), their large size permits imaging Ca waves with Ca-sensitive fluorescent dyes (23, 29, 33, 50), and Ca signaling proteins are easily expressed heterologously (7). Another important reason that *Xenopus* oocytes have been a popular system is that they have endogenous Ca-activated Cl channels, which can be used as a real-time assay for subplasmalemmal Ca (10, 25). For example, Ca-activated Cl channels have been used as an indirect measure of SOCE and for the evaluation of factors thought to regulate store-operated Ca channels (SOCs) (12, 21, 37–39).

The number of different types of Ca-activated Cl channels in the oocyte remains an open question. The pioneering studies of Miledi, Parker, Dascal, and their colleagues as well as other investigators (2, 11, 25, 30, 31, 34, 35, 44) show that responses to IP<sub>3</sub> usually consist of two or more components. An initial transient component and subsequent oscillatory components are independent of extracellular Ca and are caused by Ca release from intracellular stores. These components are followed by a sustained component, which depends on Ca influx. Yao and Parker (49) suggested that all three components are mediated by the same population of Cl channels, which are activated with different kinetics in response to Ca released from stores and by Ca influx. In contrast, Boton et al. (4) concluded that there are two different Ca-activated Cl currents because of their differential sensitivities to Ca, EGTA, and anthracene-9-carboxylic acid. We suggested that the two different Cl currents activated by Ca released from stores and Ca influx were mediated by different channels, because the currents exhibited different instantaneous current-voltage (*I-V*) and activation curves (15). Unfortunately, there are no definitive single-channel data to support the existence of two Ca-activated Cl channels. Takahashi et al. (46) reported that activation of heterologously expressed 5HT<sub>1C</sub> receptors (which activated phospholipase C) activated 3-pS Cl channels in cell-attached patches and that Ca activated the same channels in excised patches. Although another type of channel was also sometimes observed, the predominance of the 3-pS channel suggested that there was only one species of Ca-activated Cl channel in the oocyte.

Whether the different currents activated by IP<sub>3</sub> are mediated by the same or different channels, the fact that IP<sub>3</sub> stimulates currents that differ significantly in their kinetics, voltage sensitivity, sensitivity to store-released and influxed Ca, and biophysical properties is extremely interesting. If these are mediated by different channels, their differing sensitivity to the source of

The costs of publication of this article were defrayed in part by the payment of page charges. The article must therefore be hereby marked "advertisement" in accordance with 18 U.S.C. Section 1734 solely to indicate this fact.

Ca (influx from extracellular space vs. release from internal stores) suggests that differences in the amplitude or spatiotemporal features of the Ca signal from these two sources may be important in determining which channel is activated. Alternatively, if only one channel is responsible, the behavior of the Cl current must be dictated by the features of the Ca signal in intriguing ways. Because Ca-activated Cl channels have played such a prominent role in the study of Ca signaling in *Xenopus* oocytes, it is important to understand their mechanisms of regulation. The goal of the present study was to obtain additional evidence for the identity of these currents and to investigate the mechanisms of their regulation by Ca.

## METHODS

### Isolation of *Xenopus* Oocytes

Stage V-VI oocytes were harvested from adult *Xenopus laevis* females (*Xenopus* 1, Ann Arbor, MI) as described by Dascal (10). Animals were anesthetized by immersion in tricaine (1.5 g/l). Ovarian follicles were removed, cut into small pieces, and digested in normal Ringer solution with no added Ca containing 2 mg/ml collagenase type IA (Sigma Chemical, St. Louis, MO) for 2 h at room temperature. The oocytes were extensively rinsed with normal Ringer solution, placed in L-15 medium (GIBCO BRL, Gaithersburg, MD), and stored at 18°C. Oocytes were used 1–6 days after isolation.

### Electrophysiological Methods

Oocytes were voltage clamped with two microelectrodes with use of a GeneClamp 500 (Axon Instruments, Foster City, CA). Current was always recorded at maximal gain (10,000 $\times$ ) with a minimal stability setting (<200  $\mu$ s) to achieve the fastest possible voltage clamp. Electrodes were usually filled with 3 M KCl and had resistances of 0.5–2 M $\Omega$ . For the experiments in Figs. 3 and 4 with store-operated Ca current ( $I_{SOC}$ ), the electrodes were filled with 4 M potassium acetate and had resistances of 1–2 M $\Omega$ . The bath was always grounded via a 3 M KCl-agar bridge, except for experiments on  $I_{SOC}$ , in which the bath was grounded with a 4 M potassium acetate-agar bridge. Liquid junction potentials relative to Ringer solution were measured as described by Neher (27) and found to be  $-1$  mV for NaBr Ringer solution, 0 mV for NaI Ringer solution, and  $+4$  mV for *N*-methyl-D-glucamine (NMDG)-aspartate Ringer solution. Oocyte resting potentials were between  $-30$  and  $-60$  mV. Typically, the membrane was held at  $-35$  mV, stepped to  $+40$  mV for 1 s, to  $-140$  mV for 1 s, and back to  $+40$  mV for 1 s before return to the holding

potential. These steps were repeated every 10–30 s. Stimulation and data acquisition were controlled by pCLAMP6 (Axon Instruments) via a Digidata 1200 analog-to-digital-digital-to-analog converter (Axon Instruments) or Curcap32 (software and hardware developed by Bill Goolsby, Emory University). These software packages were installed in a Pentium computer. Experiments were performed at room temperature (22–26°C).

### Oocyte Injection

Oocytes were injected with various substances with use of a Nanoject Automatic Oocyte Injector (Drummond Scientific, Broomall, PA). The injection pipette was pulled from glass capillary tubing in a manner similar to that for the recording electrodes and then broken so that it had a  $<20$ - $\mu$ m-OD beveled tip. Typically, 23 nl of 1 mM IP<sub>3</sub> solution in Chelex resin-treated H<sub>2</sub>O were injected to give a calculated oocyte concentration of  $\sim 50$   $\mu$ M.

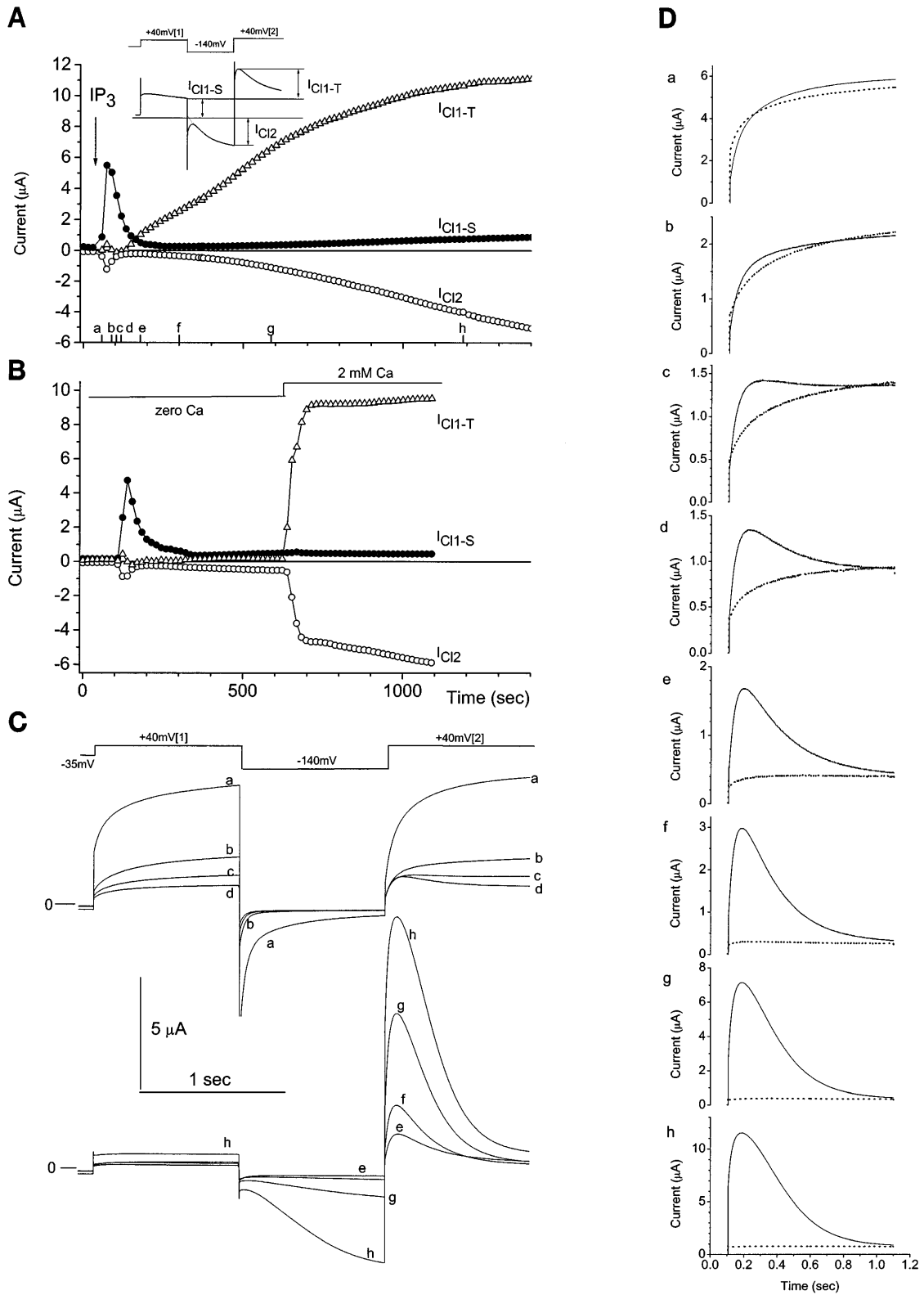
### Solutions

Normal Ringer solution consisted of (in mM) 123 NaCl, 2.5 KCl, 2 CaCl<sub>2</sub>, 1.8 MgCl<sub>2</sub>, and 10 HEPES, with pH adjusted to 7.4 with NaOH. Zero-Ca Ringer solution was the same as normal Ringer solution, except CaCl<sub>2</sub> was omitted. MgCl<sub>2</sub> was increased to 5 mM, and 0.1 mM EGTA was added. NMDG Ringer solution consisted of (in mM) 116 NMDG chloride, 2 CaCl<sub>2</sub>, 2 MgCl<sub>2</sub>, and 10 HEPES, pH 7.4. In experiments on anion permeability, 123 mM NaCl in normal Ringer solution was replaced with 123 mM NaI or NaBr. For measuring  $I_{SOC}$ , the oocytes were incubated overnight in a solution containing (in mM) 108 sodium aspartate, 1.6 potassium aspartate, 2 Ca(OH)<sub>2</sub>, 2 MgSO<sub>4</sub>, and 10 sodium HEPES, pH 7.4, before the experiment, which was conducted in Na- and Cl-free Ringer solution composed of (in mM) 113 aspartic acid, 5 calcium aspartate, and 5 HEPES, with pH adjusted to 7.4 with NMDG. Stock solutions of IP<sub>3</sub> (Sigma Chemical) were made at 10 mM in H<sub>2</sub>O, stored at  $-20^{\circ}$ C, and diluted in water to the final concentrations indicated for injection. 1,2-Bis(2-amino-phenoxy)ethane-*N,N,N,N'*-tetraacetic acid (BAPTA) potassium salt (K<sub>4</sub>BAPTA; Molecular Probes) was made at 250 mM in H<sub>2</sub>O. In all cases, injection of the same volume of water had no effect on the Cl currents. Stock solutions of A-23187 (Molecular Probes) were made in DMSO at 10 mM. Heparin (6 kDa; Sigma Chemical) was dissolved at 100 mg/ml in H<sub>2</sub>O.

### iGluR3 Expression

The rat flop form of iGluR3 cRNA was synthesized in vitro using Ambion mMessage mMachine capped RNA synthesis kit with the iGluR3 plasmid as template (accession number M85036, provided by Dr. Jim Boulter, University of Califor-

Fig. 1. Development of noninactivating outward Cl current ( $I_{Cl1-S}$ ), slow inward Cl current ( $I_{Cl2}$ ), and transient outward Cl current ( $I_{Cl1-T}$ ). A *Xenopus* oocyte was voltage clamped with 2 microelectrodes. A voltage pulse shown in *C* was applied every 10 s, and 20 nl of 1 mM inositol 1,4,5-trisphosphate (IP<sub>3</sub>) were injected at 30 s. *A*: time course of development of  $I_{Cl1-S}$ ,  $I_{Cl2}$ , and  $I_{Cl1-T}$  in response to injection of IP<sub>3</sub> to deplete endoplasmic reticulum Ca stores in an oocyte bathed in normal Ringer solution. Steady-state outward current at end of 1st  $+40$ -mV ( $+40$ -mV[1]) pulse is  $I_{Cl1-S}$  ( $\bullet$ ), inward current during  $-140$ -mV pulse is  $I_{Cl2}$  ( $\circ$ ), and transient outward current during 2nd  $+40$ -mV ( $+40$ -mV[2]) pulse is  $I_{Cl1-T}$  ( $\Delta$ ). *Inset*:  $I_{Cl1-S}$  and  $I_{Cl2}$  were plotted at end of each voltage step, and amplitude of  $I_{Cl1-T}$  was defined as difference between peak current during  $+40$ -mV[2] pulse and steady-state current at end of  $+40$ -mV[1] pulse. *B*: effect of Ca-free bathing solution on  $I_{Cl1-S}$ . Zero Ca masked development of  $I_{Cl2}$  and  $I_{Cl1-T}$ ;  $I_{Cl1-S}$  was unaffected. *C*: representative traces of  $I_{Cl1-S}$ ,  $I_{Cl2}$ , and  $I_{Cl1-T}$  at different times during experiment. Times of traces are indicated by *a–h* on *x*-axis in *A*. *Trace a*: immediately after IP<sub>3</sub> injection; time-dependent outward currents were activated during  $+40$ -mV[1] and  $+40$ -mV[2] pulses. *Traces b–d*: 1–2 min after IP<sub>3</sub> injection; note small transient outward current during  $+40$ -mV[2] pulse but not during  $+40$ -mV[1] pulse. *Traces e–h*: later times after IP<sub>3</sub>;  $I_{Cl2}$  and  $I_{Cl1-T}$  increased gradually after IP<sub>3</sub> injection. *D*: development of  $I_{Cl1-T}$  during decay of  $I_{Cl1-S}$ .  $I_{Cl1-S}$  during  $+40$ -mV[1] pulse (dashed lines) and  $I_{Cl1-T}$  (solid lines) during  $+40$ -mV[2] pulse are superimposed for each time point (*a–h*).



nia, Los Angeles). cRNA (10–23 ng) in water was injected near the equator of the oocyte 2–4 days before recording. Injection was performed as described above for IP<sub>3</sub>, and the oocytes were stored at 18°C in L-15 medium until they were used.

## RESULTS

### Time Course of Development of $I_{Cl1}$ and $I_{Cl2}$

Injection of *Xenopus* oocytes with IP<sub>3</sub> stimulates Cl currents composed of several different kinetic components (e.g., Refs. 4, 15, 30, 31, 44). Figure 1 recapitulates how we measure these currents,  $I_{Cl1-S}$ ,  $I_{Cl1-T}$ , and  $I_{Cl2}$  (15). The oocyte was voltage clamped with two microelectrodes, and the membrane potential was stepped from a holding potential of –35 to +40 mV for 1 s, –140 mV for 1 s, and +40 mV for 1 s before return to –35 mV. The first +40-mV pulse in each episode was identified as +40-mV[1] and the second +40-mV pulse as +40-mV[2]. Cl equilibrium potential ( $E_{Cl}$ ) under our conditions was about –25 mV, so that positive to this potential Cl flowed into the cell (outward current) and negative to this potential Cl flowed outward (inward current). Figure 1A plots amplitudes of three currents during this voltage protocol. Outward  $I_{Cl1}$  (called  $I_{Cl1-S}$  for “sustained”) was measured at the end of the +40-mV[1] pulse, and maximum inward  $I_{Cl2}$  was measured at the end of the –140-mV pulse. The transient outward  $I_{Cl1}$  (called  $I_{Cl1-T}$  for “transient”) is shown during the +40-mV[2] pulse. This current was calculated by measuring the maximum outward current during the +40-mV[2] pulse and subtracting the current at the end of the +40-mV[1] pulse (Fig. 1A, inset). Injection of IP<sub>3</sub> at the arrow rapidly stimulated  $I_{Cl1-S}$  (Fig. 1A), which did not inactivate during the voltage pulse. This current increased immediately after IP<sub>3</sub> injection and then declined to baseline in ~100 s. Figure 1B shows that this current did not require extracellular Ca. When  $I_{Cl1-S}$  was maximally activated (30 s after IP<sub>3</sub> injection, Fig. 1C, trace a), the currents in response to the +40-mV[1] and +40-mV[2] steps were virtually identical in waveform and amplitude.  $I_{Cl1-S}$  in response to both +40-mV pulses declined in amplitude over the next few minutes (Fig. 1C, traces b–d). As  $I_{Cl1-S}$  declined to baseline,  $I_{Cl1-T}$  in response to the +40-mV[2] pulse began to increase in amplitude (Fig. 1C, traces c–e).  $I_{Cl1-T}$  steadily increased in amplitude over the next 20 min (Fig. 1A). Figure 1D compares the currents generated by the +40-mV[1] and +40-mV[2] pulses of traces a–h. At 30 s after IP<sub>3</sub> injection,  $I_{Cl1-S}$  in response to the +40-mV[1] pulse activated slightly faster than in response to the +40-mV[2] pulse, but otherwise the currents were very similar. This difference in activation was due to the fact that some of the channels were open at the –35-mV holding potential from which the first pulse departed (15). Thus there was a time-independent current through open channels due to the increased Cl driving force in response to the +40-mV[1] pulse that was not seen in response to the +40-mV[2] pulse, which departed from –140 mV, where most of the channels were closed. In contrast, in traces b–h the

response to the +40-mV[2] pulse activated more rapidly and reached a greater peak amplitude than the response to the +40-mV[1] pulse. In traces b–h the response to the +40-mV[2] pulse inactivated to the same level as the  $I_{Cl1-S}$  current at the end of the +40-mV[1] pulse.  $I_{Cl1-T}$  did not develop if the oocyte was bathed in zero-Ca solution but developed quickly when Ca was returned to the solution (Fig. 1B). Thus  $I_{Cl1-S}$  did not require extracellular Ca, but  $I_{Cl1-T}$  did require extracellular Ca. The difference in the responses to the +40-mV[1] and +40-mV[2] pulses was due to the differences in Ca influx that occurred during the preceding voltage pulse. The +40-mV[2] pulse was preceded by a –140-mV pulse where the driving force for Ca

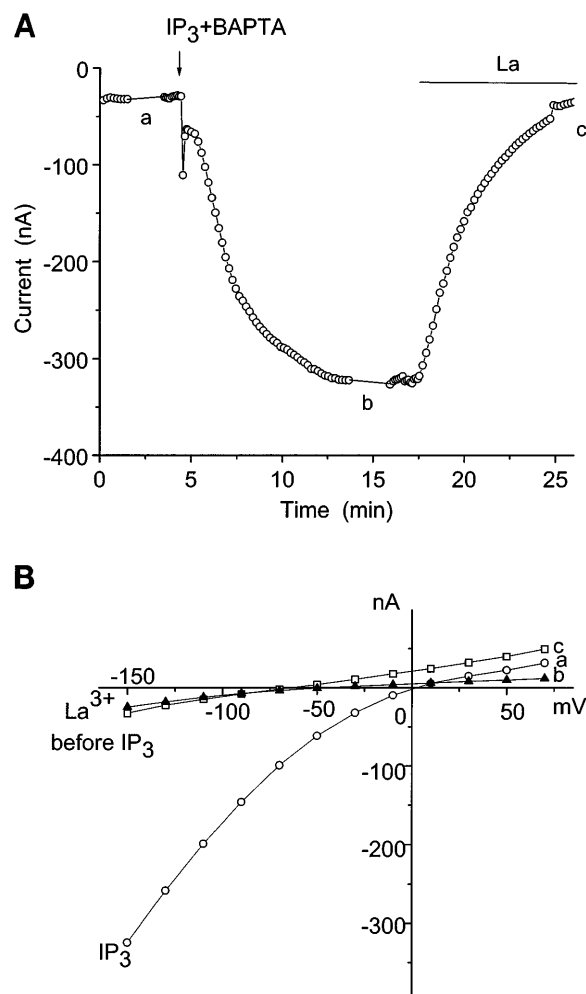


Fig. 2. A: time course of development of store-operated Ca current ( $I_{SOC}$ ). Oocyte was incubated with Cl-free solution overnight and bathed in Na- and Cl-free Ringer solution to minimize Cl currents; 46 nl of a mixture of 1 mM IP<sub>3</sub> and 100 mM 1,2-bis(2-aminophenoxy)ethane-*N,N,N,N*-tetraacetic acid (BAPTA) were injected at arrow. Immediately after injection, inward tail current of  $I_{Cl1-S}$  was evident before BAPTA could block all Cl currents (downward deflection of current at arrow). Oocyte was voltage clamped at –35-mV holding potential, and a voltage step to –140 mV for 100 ms was applied every 10 s. Inward current 10 ms after onset of –140-mV pulse was plotted vs. time. B: current-voltage ( $I$ - $V$ ) relationship before IP<sub>3</sub> injection (□), 10 min after IP<sub>3</sub> injection (○), and after application of 1 mM La (▲).

influx was high, whereas the +40-mV[1] pulse was preceded by a -35-mV holding period where Ca influx was much lower.  $I_{Cl2}$  activated more slowly than  $I_{Cl1-T}$  (Fig. 1A).  $I_{Cl2}$  seldom became fully activated during the

typical 20- to 30-min experiment.  $I_{Cl2}$ , like  $I_{Cl1-T}$ , was also dependent on extracellular Ca (Fig. 1B).  $I_{Cl2}$  activated slowly with a sigmoidal time course during the -140-mV pulse.

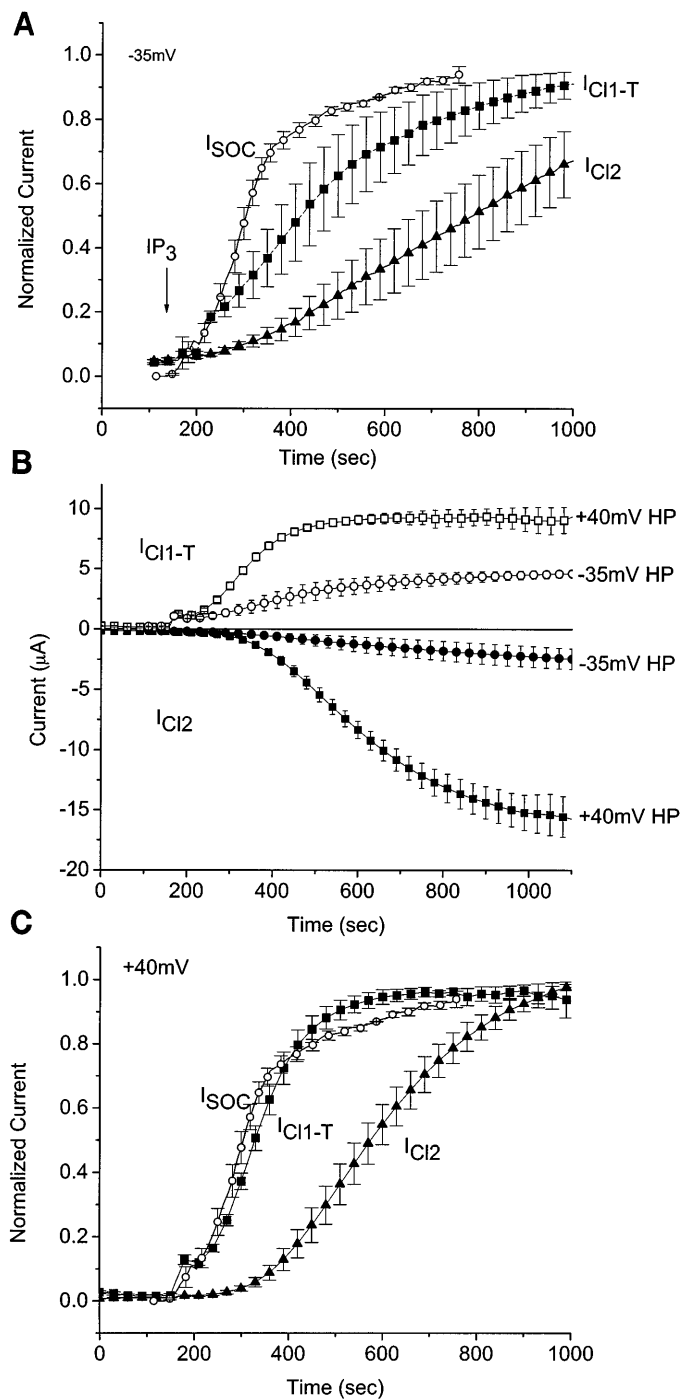


Fig. 3. Time course of development of  $I_{Cl2}$  and  $I_{Cl1-T}$  compared with  $I_{SOC}$ . **A**: amplitudes of currents were normalized and plotted vs. time. Maximum currents (1.0) corresponded to  $-275 \pm 57$  nA ( $n = 5$ ) for  $I_{SOC}$ ,  $3.3 \pm 0.8$   $\mu A$  for  $I_{Cl1-T}$  ( $n = 4$ ), and  $-0.55 \pm 0.1$   $\mu A$  ( $n = 4$ ) for  $I_{Cl2}$ . Currents were measured from same batch of oocytes. **B**: dependence of development of  $I_{Cl2}$  and  $I_{Cl1-T}$  on holding potential. Currents were measured using standard voltage-clamp protocol described in Fig. 1 legend, except holding potential was either -35 or +40 mV. **C**: amplitudes of currents in **B** at +40-mV holding potential normalized and plotted vs.  $I_{SOC}$  from **A**.

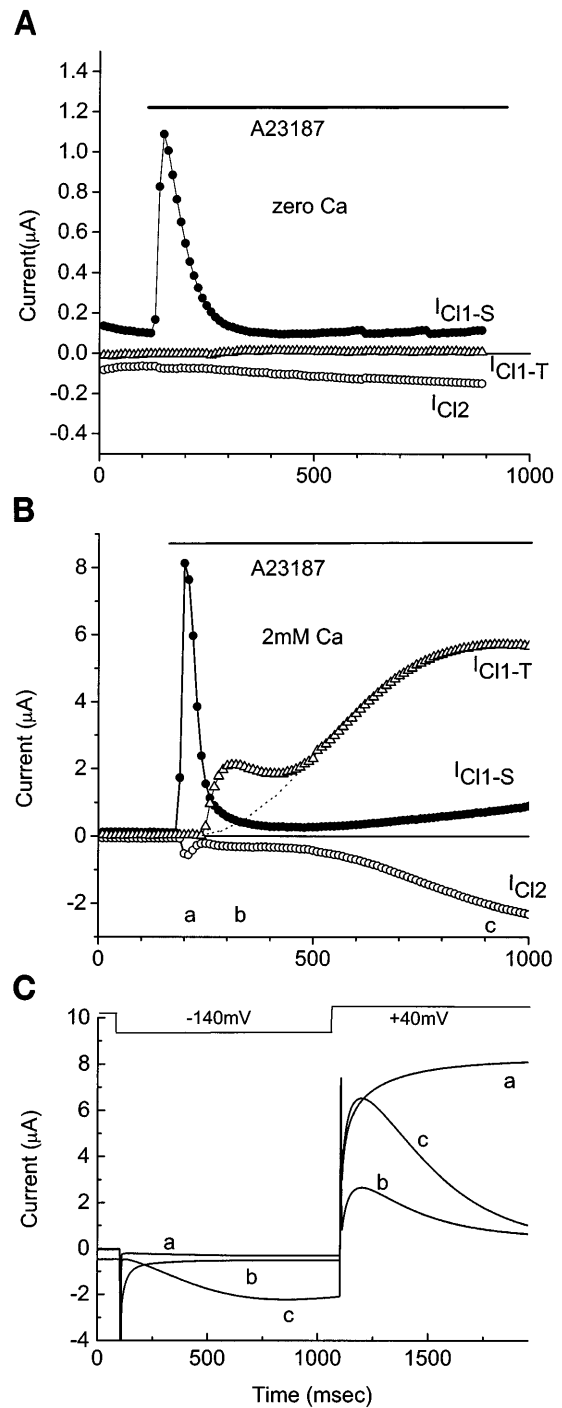
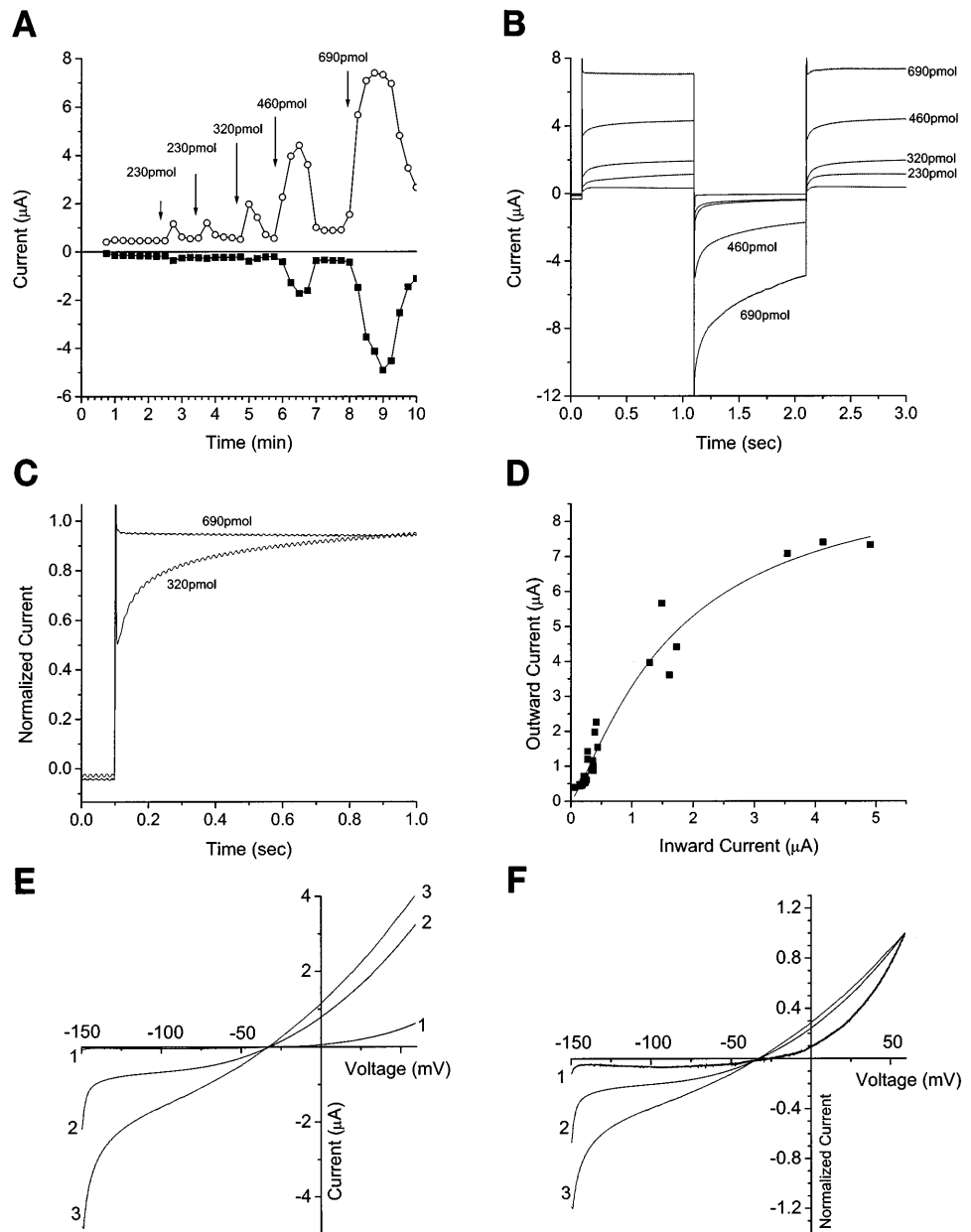


Fig. 4. Ca ionophore A-23187 stimulates Ca release from stores and Ca influx. **A**: 0.5  $\mu M$  A-23187 was applied to oocyte in zero-Ca Ringer solution. Experimental conditions as described in Fig. 1 legend. A-23187 activated  $I_{Cl1-S}$ , but  $I_{Cl2}$  and  $I_{Cl1-T}$  did not develop. **B**: A-23187 was applied to oocyte in normal Ringer solution (2 mM Ca).  $I_{Cl1-S}$  developed normally, but  $I_{Cl1-T}$  developed in a biphasic manner, which was not observed in response to  $IP_3$  injection (e.g., Figs. 1 and 3).  $I_{Cl2}$  development was delayed until 2nd phase of  $I_{Cl1-T}$  development had begun. Dashed line, development of  $I_{Cl1-T}$  as result of store-operated Ca entry. **C**: actual current traces (a-c) corresponding to **B**.

Fig. 5. Effects of Ca injection on Cl currents in *Xenopus* oocytes. **A**: oocytes were voltage clamped, and voltage pulses were applied as described in Fig. 4 legend.  $\circ$ , Outward current at end of +40-mV[1] pulse;  $\blacksquare$ , inward current at end of -140-mV pulse.  $\text{CaCl}_2$  (230–690 pmol) was injected at times indicated. **B**: representative traces corresponding to responses in **A**. **C**: comparison of time course of outward currents during +40-mV[1] pulse in response to injection of 320 pmol or 690 pmol Ca. Currents in **B** were normalized and superimposed. **D**: relationship of inward and outward currents in experiment in **A**. **E**:  $I$ - $V$  relationships obtained after injection of different amounts of Ca.  $I$ - $V$  relationships were determined by a 5-s ramp from -140 to +60 mV from a holding potential of -35 mV. Numbers at ends of curves indicate number of 23-nl pulses of 10 mM  $\text{CaCl}_2$  injected. **F**: normalized  $I$ - $V$  relationships.  $I$ - $V$  relationships in **E** were normalized to same value at +60 mV. Numbers on *left* correspond to number of 23-nl 10 mM Ca injections. Reversal potentials were close to Cl equilibrium potential.



#### Relationship of Cl Channel Activation to $I_{\text{SOC}}$ Activation

In Fig. 1A,  $I_{\text{Cl}_2}$  developed more slowly than  $I_{\text{Cl}_1\text{-T}}$ . This observation suggested that these two currents were activated differently and raised the question of how the development of these currents related to the development of SOCE. To examine this question, we measured  $I_{\text{SOC}}$  directly, as we previously described (15). The oocytes were incubated in Cl-free solution overnight to deplete cytosolic Cl, and the experiments were performed in Cl-free solutions to minimize Cl currents. In addition,  $I_{\text{SOC}}$  was isolated by blocking Ca-activated Cl currents by injection of BAPTA (5 mM oocyte concentration). Under these conditions, injection of  $\text{IP}_3$  or treatment with thapsigargin resulted in the development of an inwardly rectifying current that was blocked by La

or removal of extracellular Ca (Fig. 2). On average,  $I_{\text{SOC}}$  developed with a half time of  $\sim 100$  s.

The time course of development of  $I_{\text{SOC}}$  is compared with the development of  $I_{\text{Cl}_1\text{-T}}$  and  $I_{\text{Cl}_2}$  measured by our standard +40-mV, -140-mV pulse, -35-mV holding potential protocol in Fig. 3A. Surprisingly, the time course of development of  $I_{\text{Cl}_1\text{-T}}$  and  $I_{\text{Cl}_2}$  lagged significantly behind the development of  $I_{\text{SOC}}$ . We hypothesized that the lag between the development of  $I_{\text{SOC}}$  and Cl currents might be related to the difference in conditions for measuring  $I_{\text{SOC}}$  (high intracellular BAPTA) and for measuring Cl currents. By reducing the level of cytosolic Ca, BAPTA could accelerate the development of  $I_{\text{SOC}}$  by reducing its inactivation by Ca (18, 53) and by reducing deactivation of  $I_{\text{SOC}}$  due to partial refilling of Ca stores. We tested this idea by changing Ca influx by

holding the oocyte at different potentials (Fig. 3B). The development of  $I_{Cl1-T}$  and  $I_{Cl2}$  was strongly affected by holding potential. With a +40-mV holding potential, both currents developed more quickly and became larger than with the -35-mV holding potential. Because one would expect that Ca influx during the holding period would be less at +40 mV than at -35 mV, this supports the suggestion that the development of  $I_{SOC}$  varies with the availability of cytosolic Ca. With the +40-mV holding potential the development of  $I_{SOC}$  corresponded almost precisely with the development of  $I_{Cl1-T}$  (Fig. 3C). In contrast, the development of  $I_{Cl2}$  remained considerably slower. The correspondence of  $I_{SOC}$  and  $I_{Cl1-T}$  development in Fig. 3C might be coincidental, but the important point is that the time course of development of  $I_{Cl1-T}$  and  $I_{Cl2}$  differs significantly at both holding potentials tested. This difference suggests that these two currents are regulated differently.

These observations raised several questions. Are  $I_{Cl1-S}$ ,  $I_{Cl1-T}$ , and  $I_{Cl2}$  mediated by the same or by different channels? Do the different currents have the same or different sensitivity to Ca? Why is  $I_{Cl2}$  apparently not activated in response to Ca released from stores? Do the waveforms of  $I_{Cl2}$  and  $I_{Cl1-T}$  simply reflect subplasmalemmal Ca concentration, or is there a more complex relationship between Ca and channel activation? Why does  $I_{Cl1-S}$  turn off within several minutes after  $IP_3$  injection?

#### Activation of $I_{Cl2}$ by Ca Injection and Influx

To test whether the slow development of  $I_{Cl2}$  involved a time-dependent activation of some metabolic process, we examined whether it was possible to activate  $I_{Cl2}$  by

Ca influx through other types of Ca channels. We predicted that if  $I_{Cl2}$  activation required some time-dependent process subsequent to Ca influx, this process should occur with similar kinetics regardless of the method of elevation of subplasmalemmal Ca.

*A-23187.* Initially, we tried to produce Ca influx directly via Ca ionophores such as A-23187 or ionomycin, but the interpretation was complicated, because A-23187 and ionomycin produced massive and immediate release of Ca from internal stores, as reported previously (4, 26, 48, 51). A-23187 stimulated  $I_{Cl1-S}$  in the absence of extracellular Ca in the same way that  $IP_3$  injection did (Fig. 4A), showing that it released Ca from intracellular stores. In the presence of extracellular Ca,  $I_{Cl1-T}$  developed in a distinctively biphasic manner (Fig. 4B). A-23187 resulted in a rapid initial increase in  $I_{Cl1-T}$  (the "hump" in the curve between 200 and 500 s) followed by a slower sigmoidal increase (approximated by the dashed line between 200 and 500 s). The hump was due to Ca influx through A-23187 channels in the plasma membrane, because it was never seen with  $IP_3$  injection. Although  $I_{Cl1-T}$  was activated by Ca influx through A-23187 channels,  $I_{Cl2}$  was not activated appreciably during this time period.  $I_{Cl2}$  did activate later (>500 s), however, as SOCE developed as a consequence of depletion of Ca stores by A-23187. The observation that  $I_{Cl2}$  was not activated by Ca influx through A-23187 channels suggested that  $I_{Cl1-T}$  and  $I_{Cl2}$  were regulated differently by Ca.

*Ca injection.* We also activated Ca-activated Cl currents by direct injection of Ca into the oocyte. The amount of Ca required to activate the Cl currents

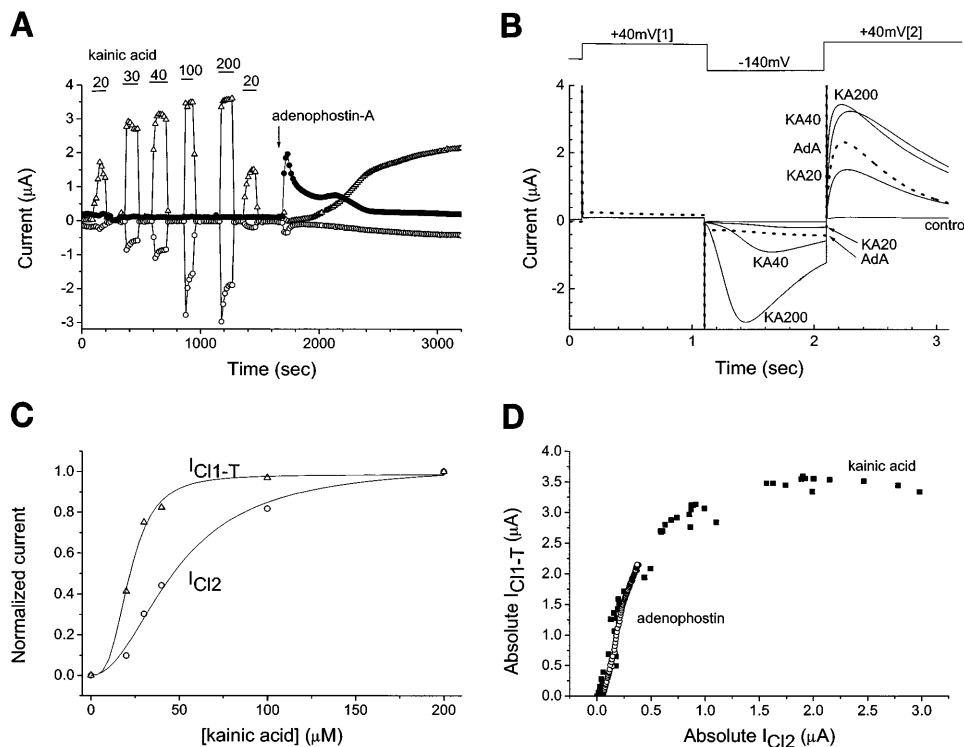


Fig. 6. Activation of  $I_{Cl1-S}$  by Ca influx mediated by ionotropic glutamate receptor iGluR3. An oocyte injected 3 days previously with 23 ng of iGluR3 cRNA was bathed in Ringer solution in which Na was replaced with *N*-methyl-D-glucamine (NMDG). *A:* kainic acid (20–200 μM in normal Ringer solution) was applied to bath as indicated by horizontal bars. After dose-response curve to kainic acid was established, 23 nl of 10 μM adenophostin A were injected into oocyte.  $\Delta$ ,  $I_{Cl1-T}$ ;  $\circ$ ,  $I_{Cl2}$ ;  $\bullet$ ,  $I_{Cl1-S}$ . *B:* representative current traces from experiment in *A* in presence of 20, 40, and 200 μM kainic acid (KA20, KA40, and KA200, respectively; solid traces) and 10 min after adenophostin A (AdA) injection (dashed trace). *C:* dose-response curve for kainic acid. Amplitudes of  $I_{Cl1-T}$  ( $\Delta$ ) and  $I_{Cl2}$  ( $\circ$ ) were plotted vs. kainic acid concentration for experiment in *A*. Virtually identical results were obtained from 6 cells. *D:* comparison of amplitudes of  $I_{Cl1-T}$  and  $I_{Cl2}$ .  $I_{Cl1-T}$  and  $I_{Cl2}$  amplitudes were plotted vs. each other for each episode of experiment in *A*.  $\blacksquare$ , Kainic acid;  $\circ$ , adenophostin A.

depended critically on the depth and hemispheric location of the injection pipette, as reported previously (25). Figure 5 shows a typical result. Injection of  $\sim 230$  pmol of Ca into the oocyte elicited an outward current that activated slowly on depolarization and exhibited a time-dependent deactivating tail current on hyperpolarization (Fig. 5, *A* and *B*; 230 and 320 pmol). Very little inward current was present at the end of the 1-s pulse at  $-140$  mV with these small Ca injections. In contrast, larger injections of Ca (460–690 pmol) activated outward currents that exhibited little or no time-dependent activation (Fig. 5, *B* and *C*; cf. time course of currents stimulated by 320 and 690 pmol Ca) and stimulated large inward currents (Fig. 5, *A* and *B*; 460 and 690 pmol). Figure 5*D* shows that the relationship between inward and outward current induced by Ca injection is nonlinear. Outward currents up to  $\sim 2$   $\mu$ A in amplitude were associated with only small inward currents. These data suggest that inward currents may be less sensitive to Ca than outward currents. The different Ca sensitivity of inward and outward currents is confirmed in Fig. 5, *E* and *F*, which shows the *I-V* relationships in response to different Ca injections. In this experiment, multiple 23-nl injections of 10 mM Ca were made as in Fig. 5*A*. The *I-V* relationships were determined by 5-s-duration linear ramps from  $-140$  to  $+60$  mV. It should be emphasized that these *I-V* relationships are neither instantaneous nor steady state, and their shapes are influenced by the waveform of time-dependent currents. Nevertheless, we chose to use a ramp protocol, rather than a step protocol, so that we could obtain an approximation of the steady-state *I-V* relationship in a short period of time while the Ca concentration was (presumably) not changing significantly. A single bolus of 23 nl stimulated only outward current and no measurable inward current (Fig. 5*E*, trace 1). Two boluses (Fig. 5*E*, trace 2) injected in quick succession stimulated more outward current but also stimulated significant inward current. Three boluses (Fig. 5*E*, trace 3) increased the outward current only a small amount over that evoked by two boluses but stimulated inward current twofold. The amount of inward current relative to the amount of outward current became greater with increasing amounts of Ca injected. This is shown in Fig. 5*F*, where the traces are normalized to the same amount of outward current at  $+60$  mV. As increasing amounts of Ca were injected, significantly more inward current was recorded and the curves become less outwardly rectifying.

**Expressed *iGluR3* Ca channels.** The experiments in Fig. 5 suggested that the inward Cl current stimulated by Ca injection was less sensitive to Ca than outward current. Is this inward current the same as  $I_{Cl2}$ ? The waveform of the inward current induced by Ca injection was very different from that of  $I_{Cl2}$ , but it is possible that the waveform of  $I_{Cl2}$  is determined by the dynamics of the Ca signal rather than by some intrinsic property of the Cl channel itself. If  $I_{Cl2}$  is mediated by the same pathway as the inward current induced by Ca injection, we would expect that  $I_{Cl2}$  would have a lower Ca sensitivity than  $I_{Cl1-T}$ . To test whether  $I_{Cl2}$  and  $I_{Cl1-T}$

have different Ca sensitivities, we examined Cl currents stimulated by Ca influx through the ionotropic glutamate receptor *iGluR3*, a ligand-gated ion channel that exhibits a high Ca permeability (5). cRNA for *iGluR3* was injected into the oocyte several days before the experiment. The oocyte was bathed in a solution in which the only permeant cation present was Ca (Na was replaced with NMDG). In the absence of a glutamate receptor agonist, the currents in *iGluR3* oocytes were essentially identical to those in uninjected oo-

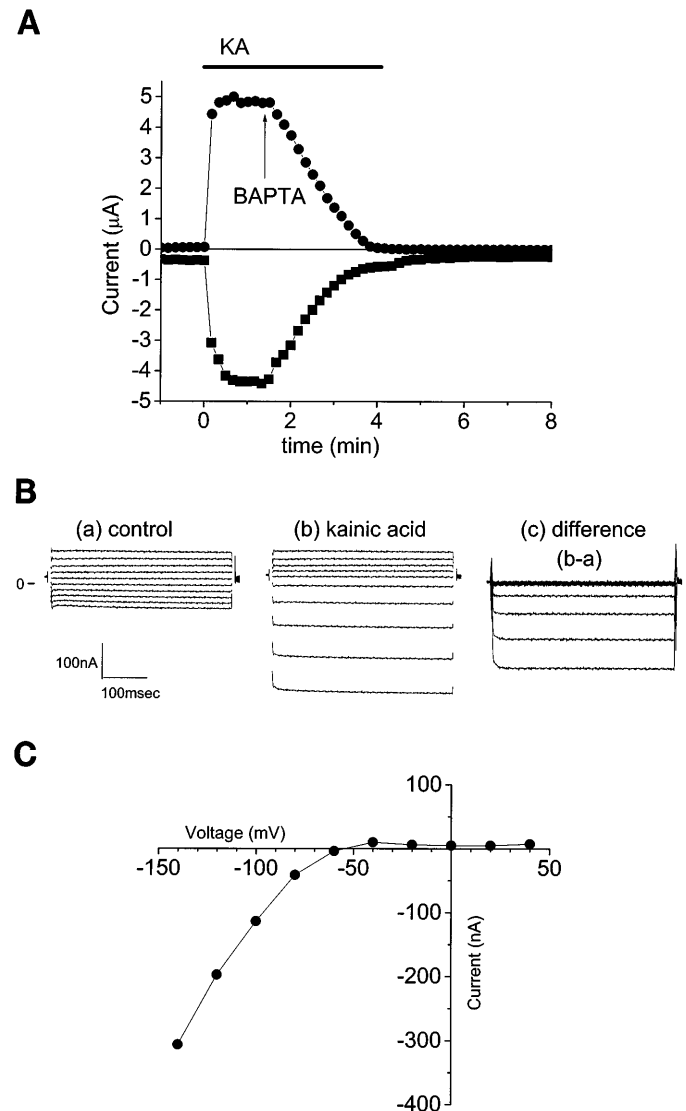


Fig. 7. Isolation of Ca current through glutamate receptor (*GluR3*) channels. *A*: *iGluR3* cRNA-injected oocyte was bathed in NMDG Ringer solution and voltage clamped as described in Fig. 6 legend.  $I_{Cl1-T}$  ( $\bullet$ ) and  $I_{Cl2}$  ( $\blacksquare$ ) appeared immediately after oocyte was exposed to 100  $\mu$ M kainic acid (KA). BAPTA (9.2 nl of 250 mM) was then injected, and current declined significantly as Ca-activated Cl currents were inhibited. Current that remained was largely Ca current through *iGluR3* receptor. Current disappeared when kainic acid was washed out. *B*: *I-V* relationships of *iGluR3* current. At 8 min after BAPTA injection to block Cl currents, voltage steps ( $-140$  to  $+40$  mV, 20-mV steps) were applied in presence (*b*) and absence (*a*) of kainic acid; *c*, kainic acid-sensitive currents obtained by subtracting trace *a* from trace *b*. *C*: steady-state *I-V* relationship of kainic acid-sensitive currents from trace *c* in *B*.

cytes. However, addition of the iGluR3 agonist kainic acid activated Cl currents (Fig. 6A). Although kainic acid did not stimulate  $I_{Cl1-S}$  (Fig. 6A and +40-mV[1] pulse in Fig. 6B), it did stimulate  $I_{Cl1-T}$  and  $I_{Cl2}$  (Fig. 6A and -140-mV and +40-mV[2] pulses in Fig. 6B). Low concentrations of kainic acid activated  $I_{Cl1-T}$  preferentially, whereas higher concentrations activated  $I_{Cl1-T}$  and  $I_{Cl2}$ . Another important observation was that  $I_{Cl1-T}$  and  $I_{Cl2}$  increased maximally within 10 s after application of kainic acid. Although this experiment did not exclude the involvement of a metabolic step in activation of these Cl currents, it did demonstrate that the ~10 min typically required for  $I_{Cl2}$  activation (Fig. 3B) were unlikely to be due to a slow metabolic step.

If we assume that the amount of Ca influx is related to the dose of kainic acid used to activate the channel, a plot of the amplitude of  $I_{Cl1-T}$  and  $I_{Cl2}$  as a function of kainic acid concentration will show the relative Ca sensitivity of these two currents to Ca concentration. Figure 6C shows that  $I_{Cl1-T}$  is approximately twice as sensitive to kainic acid as  $I_{Cl2}$  ( $EC_{50} = 22 \mu\text{M}$  for  $I_{Cl1-T}$  and  $47 \mu\text{M}$  for  $I_{Cl2}$ ). As discussed above, we can exclude the hypothesis that  $I_{Cl2}$  activation requires intermediate steps that require a long time to activate, because kainic acid stimulates  $I_{Cl2}$  as rapidly as it activates  $I_{Cl1-T}$  (Fig. 6A). The simplest explanation for these data, then, is that  $I_{Cl1-T}$  channels are more sensitive to Ca and saturate at lower Ca concentration than do the channels responsible for  $I_{Cl2}$ . This is illustrated in a different way in Fig. 6D, where  $I_{Cl1-T}$  is plotted vs. the amplitude of  $I_{Cl2}$  for each voltage-clamp episode for the duration of the experiment. The relationship in response to kainic acid is shown in Fig. 6D. These data show there was little  $I_{Cl2}$  associated with  $I_{Cl1-T}$  amplitudes  $< 2 \mu\text{A}$ .

A nonlinear relationship between  $I_{Cl1-T}$  and  $I_{Cl2}$  is also found in response to  $\text{IP}_3$  or adenophostin A. In Fig. 6A, after we had determined the concentration-response curve for kainic acid, we injected the oocyte with adenophostin, which we previously showed releases Ca from internal stores, produces Ca influx, and activates  $I_{Cl1-T}$  and  $I_{Cl2}$  (16). Adenophostin activated  $I_{Cl1-T}$  and  $I_{Cl2}$  to about the same level that  $20 \mu\text{M}$  kainic acid did. In Fig. 6D, the relationship between  $I_{Cl1}$  and  $I_{Cl2}$  after adenophostin injection is shown. These data are superimposed on those obtained with the kainic acid data, suggesting that the small increase in  $I_{Cl2}$  after adenophostin injection can be explained simply by a lower apparent sensitivity of  $I_{Cl2}$  to Ca. The apparent higher Ca sensitivity of  $I_{Cl1-T}$  than of  $I_{Cl2}$  was also obvious when the cell was injected with  $\text{IP}_3$  (not shown).

In Fig. 6, clearly some of the inward current would be expected to be due to Ca flux through the iGluR3 channel itself. To determine the extent to which the Cl currents in Fig. 6 were contaminated with Ca current through the iGluR3 channel, we measured the iGluR3 Ca current in Fig. 7. In Fig. 7, an oocyte expressing iGluR3 was exposed to kainic acid, which stimulated an inward and an outward current. Subsequent injection of BAPTA (calculated final concentration  $2.5 \text{ mM}$ ) to block Ca-activated Cl currents caused a large decrease in the inward and outward currents. The inwardly rectifying current that remained was dependent on the presence of kainic acid and was due to Ca current through the iGluR3 channel. These data show that the amplitude of the inward current at the end of the -140-mV pulse with the maximal kainic acid concentration tested was  $< 10\%$  of the amplitude of  $I_{Cl2}$  and did not contribute to the outward current.

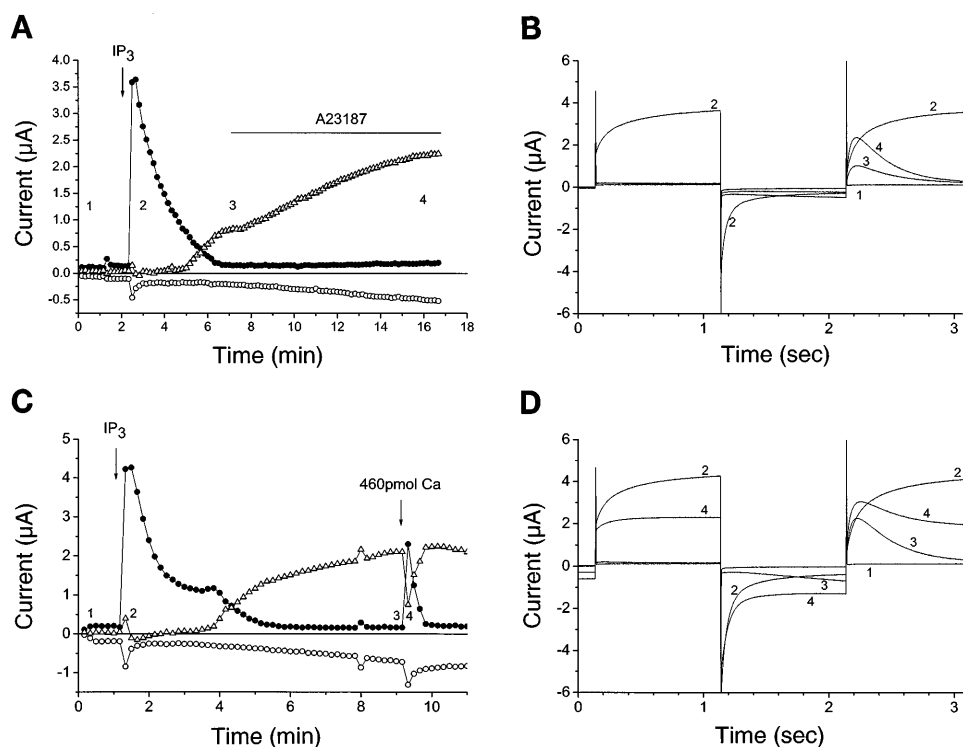


Fig. 8. Mechanism of turnoff of  $I_{Cl1-S}$ . **A:** A-23187 does not stimulate  $I_{Cl1-S}$  after  $\text{IP}_3$  injection has depleted Ca stores.  $\text{IP}_3$  (23 nl of 10 mM) was injected, and  $5 \mu\text{M}$  A-23187 was added to bath as indicated.  $\circ$ ,  $I_{Cl2}$ ;  $\bullet$ ,  $I_{Cl1-S}$ ;  $\triangle$ ,  $I_{Cl1-T}$ . **B:** current traces from experiment in A. Numbers (1-4) correspond to times in A. **C:** injection of Ca after  $\text{IP}_3$  injection stimulates  $I_{Cl1-S}$ .  $\text{IP}_3$  (23 nl of 10 mM) was injected, and 460 pmol of Ca were injected as indicated. **D:** current traces from experiment in A. Numbers correspond to times in B.

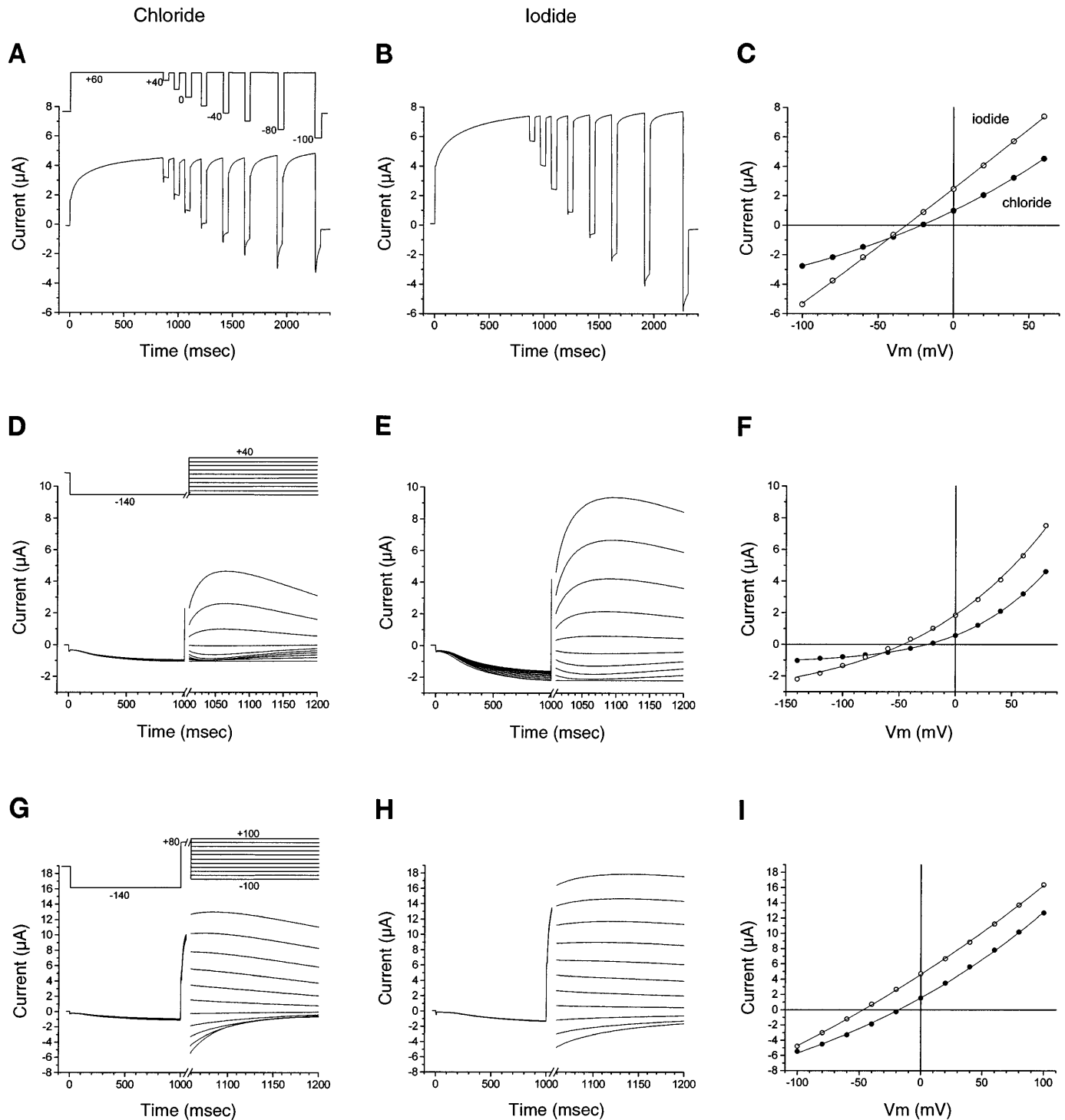


Fig. 9. Ionic selectivity of  $I_{Cl1-S}$ ,  $I_{Cl2}$ , and  $I_{Cl1-T}$ . Reversal potentials of  $I_{Cl1-S}$ ,  $I_{Cl2}$ , and  $I_{Cl1-T}$  were determined by plotting instantaneous  $I-V$  relationships in normal Ringer solution (133.5 mM Cl; A, D, and G), iodide Ringer solution (123 mM I, 10.5 mM Cl; B, E, and H), and bromide Ringer solution (not shown; see Table 1 for average reversal potentials and calculated anion selectivities). A-C:  $I_{Cl1-S}$ . Oocyte was stepped to +60 mV, then subjected to short repolarizations of 50 ms to different test potentials between +40 and -100 mV in normal Ringer solution. This protocol was repeated every 5 s, and  $IP_3$  was injected to stimulate  $I_{Cl1-S}$  (A). Then oocyte was switched to 123 mM iodide solution, and  $I-V$  curve in response to same protocol was obtained (B). Current at 9 ms after start of test pulse was plotted as a function of test potential (C). ●, Cl; ○, I. D-F:  $I_{Cl2}$ . Oocyte was bathed in normal Ringer solution for ~15 min after  $IP_3$  injection. Then a 1-s duration pulse to -140 mV followed by 1-s test pulse to different potentials was applied (D). Bath was replaced with iodide Ringer solution, and same pulses were repeated (E). F:  $I-V$  plot. G-I:  $I_{Cl1-T}$ . At ~15 min after  $IP_3$  injection, oocyte was stepped to -140 mV for 1 s to stimulate Ca influx and then to +80 mV for 50 ms to elicit  $I_{Cl1-T}$ ; this was followed by different test potentials in normal (G) and iodide (H) Ringer solution. I:  $I-V$  plot.

*Mechanism of Turnoff of  $I_{Cl-S}$*

Figures 5 and 6 show that outward Cl current is generally more sensitive to Ca than is inward Cl current. If this is true, the following questions arise: Why does  $I_{Cl-S}$  inactivate so quickly after IP<sub>3</sub> injection (Fig. 1A)? Is  $I_{Cl-S}$  a unique Cl current that has intrinsic inactivating properties, or does the turnoff reflect the decline in the Ca signal? The data in Fig. 8 show that the inactivation of  $I_{Cl-S}$  is due to depletion of Ca from internal stores and is not intrinsic inactivation of the Cl channel. Several minutes after IP<sub>3</sub> injection when  $I_{Cl-S}$  has turned off, bath application of ionomycin (not shown) or A-23187 (Fig. 8, A and B) does not stimulate  $I_{Cl-S}$ . However, injection of Ca does significantly stimulate outward current, which resembles  $I_{Cl-S}$  (Fig. 8, C and D). Because Ca is able to activate  $I_{Cl-S}$ , the Cl channel clearly is not inactivated and can be stimulated when Ca is provided. The inability of A-23187 to stimulate this current, however, suggests that the stores do not contain sufficient Ca to activate the Cl channels. We have shown in Fig. 4 that A-23187 does stimulate a large  $I_{Cl-S}$  when applied before IP<sub>3</sub> injection, showing that A-23187 is capable of releasing enough Ca from stores to activate the current, provided the stores are filled with Ca. These results show that  $I_{Cl-S}$  turns off after IP<sub>3</sub> injection, because Ca release from stores has waned, but SOCE has not yet completely developed. When SOCE has developed, the waveform of the current will be dependent on the voltage dependence of Ca influx and efflux.

*Are  $I_{Cl1}$  and  $I_{Cl2}$  Due to One or Multiple Channel Types?*

The data presented so far show that the inward Ca-activated Cl current is less sensitive to Ca than is the outward current. This could be explained 1) if there were two different Cl channels having different sensitivities to Ca and different biophysical properties or 2) if the Ca sensitivity and biophysical properties of a single Cl channel were voltage dependent. For example, if hyperpolarization decreased the Ca sensitivity of the channel, more Ca would be required to activate it.

To gain additional information about whether  $I_{Cl-S}$ ,  $I_{Cl-T}$ , and  $I_{Cl2}$  were mediated by different channels, we examined their ionic selectivity. The reversal potentials of the instantaneous *I-V* relationships for  $I_{Cl-S}$ ,  $I_{Cl2}$ , and  $I_{Cl-T}$  were measured as described previously (15) with

Cl, I, or Br as the charge-carrying species in the extracellular solution. Figure 9 shows typical current traces for 133.5 mM Cl and 123 mM I for  $I_{Cl-S}$  (A and B),  $I_{Cl2}$  (D and E), and  $I_{Cl-T}$  (G and H). The instantaneous *I-V* relationships in Cl and I are shown. Table 1 summarizes the measured reversal potentials and calculated anion-to-Cl permeability ratios. For all three currents, the order of ion selectivity was the same: I > Br > Cl. However, there were quantitative differences between the currents. The I-to-Cl permeability ratio ( $P_I/P_{Cl}$ ) for  $I_{Cl-S}$  was only about one-half of that of  $I_{Cl-T}$  and  $I_{Cl2}$ . The differences between  $I_{Cl2}$  and  $I_{Cl-T}$ , however, were insignificant: the Br-to-Cl permeability ratios were the same, and  $P_I/P_{Cl}$  values were statistically different only at the 0.04 level. These data suggest that two different channels may exist.

*Ca-Induced Ca Release and  $I_{Cl-T}$*

Other investigators who believe that  $I_{Cl-T}$  and  $I_{Cl2}$  are the same current (36, 50) argue that the current we call  $I_{Cl-T}$  is actually due to reactivation of  $I_{Cl2}$  resulting from Ca release from the ER induced by Ca influx during the previous hyperpolarizing pulse. To test this hypothesis, we injected oocytes with a large concentration of heparin to block Ca release from the ER after  $I_{Cl2}$  was fully activated to determine whether  $I_{Cl-T}$  could be explained by Ca-induced Ca release (Fig. 10). We first tested whether heparin could block IP<sub>3</sub>-induced Ca release. In Fig. 10A, a concentration of IP<sub>3</sub> was injected that released Ca from stores and activated SOCE and  $I_{Cl2}$ . After ~20 min, presumably as the IP<sub>3</sub> was hydrolyzed, the Cl currents returned to baseline levels as Ca stores became refilled (16). Heparin was then injected. A second injection of IP<sub>3</sub> after the heparin injection produced no effect as a result of blockage of IP<sub>3</sub> receptors by heparin. Heparin was also able to block Ca oscillations very quickly (Fig. 10B). Low concentrations of IP<sub>3</sub> stimulated  $I_{Cl-S}$  oscillations (16), which were blocked within 1 min after heparin injection. In contrast (Fig. 10C), injection of heparin after  $I_{Cl-T}$  and  $I_{Cl2}$  had fully developed usually increased ( $n = 5$ ) but never decreased  $I_{Cl-T}$  and  $I_{Cl2}$ . We have not investigated the mechanism of the stimulatory effect of heparin. Nevertheless, these data show that  $I_{Cl-T}$  does not require Ca-induced Ca release.

Table 1. Anionic selectivity of Cl channels in *Xenopus* oocytes

Current	$E_{rev}$ , mV				$P_{Br}/P_{Cl}$	$P_I/P_{Cl}$
	Cl → Br	Cl → I	Cl → Br	Cl → I		
$I_{Cl-S}$	-26.3 ± 0.5	-33.8 ± 0.5	-23.5 ± 0.8	-31.9 ± 0.6	1.37 ± 0.02 (5)	1.42 ± 0.03 (7)
$I_{Cl2}$	-27.1 ± 2.0	-39.1 ± 3.2	-22.9 ± 1.0	-48.2 ± 1.9	1.66 ± 0.08† (7)	2.84 ± 0.17* (6)
$I_{Cl-T}$	-23.1 ± 0.7	-36.3 ± 0.9	-17.3 ± 0.9	-46.8 ± 0.4	1.73 ± 0.04* (7)	3.36 ± 0.10*† (6)

Values are means ± SE.  $I_{Cl-S}$ , noninactivating outward Cl current;  $I_{Cl2}$ , slow outward Cl current;  $I_{Cl-T}$ , transient outward Cl current. Numbers in parentheses are numbers of oocytes. Reversal potentials ( $E_{rev}$ ) of currents were measured as described in Fig. 9 legend with 133.5 mM extracellular Cl or 123 mM extracellular I or Br with 10.5 mM Cl. Permeability ratios ( $P_{Br}/P_{Cl}$  and  $P_I/P_{Cl}$ ) were calculated pairwise for each oocyte by using Goldman-Hodgkin-Katz equation (17). \* Statistically different from  $I_{Cl-S}$ ,  $P = 0.01$ . † Statistically different from value in line immediately above,  $P = 0.04$ .

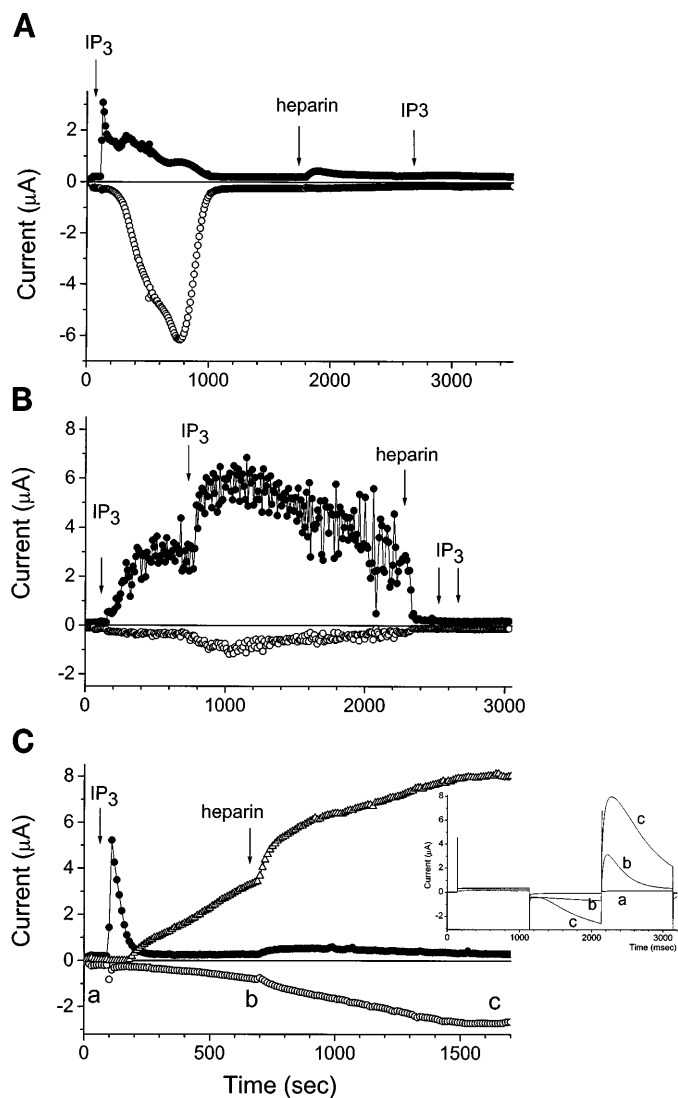


Fig. 10. Effect of heparin on Cl currents. Oocyte was voltage clamped by a 1-s pulse to  $-140$  mV followed by a 1-s pulse to  $+40$  mV from a holding potential of  $-35$  mV. *A*: heparin blocks response to  $IP_3$ .  $IP_3$  (46 nl of  $10 \mu M$ ) was injected into a voltage-clamped oocyte. Inward and outward currents were plotted as described in Fig. 1 legend.  $IP_3$  activated  $I_{Cl1-S}$  (●) and  $I_{Cl2}$  (○). After heparin (46 nl of  $100$  mg/ml) had been injected (arrow), oocyte did not respond to same amount of  $IP_3$ . Repeated injections of this concentration of  $IP_3$  are able to induce  $I_{Cl1-S}$  if heparin is not injected (16). *B*: heparin blocks Ca oscillations in response to low concentration of  $IP_3$ .  $IP_3$  (23 nl of  $10 \mu M$ ) produced oscillations of  $I_{Cl1-S}$  in this oocyte. Subsequent injection of heparin arrested oscillations. *C*: heparin has no effect on activation of  $I_{Cl1-T}$  after stores have been depleted. Heparin was injected after  $IP_3$  (23 nl of  $1$  mM) injection depleted Ca stores. *Inset*: current traces before and after heparin injection.

## DISCUSSION

We showed previously (15, 24) that *Xenopus* oocytes develop three different Ca-activated Cl currents after  $IP_3$  injection.  $I_{Cl1-S}$  is activated by Ca released from stores, and  $I_{Cl1-T}$  and  $I_{Cl2}$  are activated in a transient manner by Ca influx. The present studies provide additional insights into the mechanisms of regulation of these currents. We show here that  $I_{Cl2}$  is less sensitive to Ca than is  $I_{Cl1-S}$  or  $I_{Cl1-T}$ . This difference in

sensitivity of these currents to Ca provides a plausible explanation for why Ca release from stores does not activate  $I_{Cl2}$ : the level of Ca released from stores may be below threshold for  $I_{Cl2}$  activation. If we assume that  $I_{Cl1-S}$  and  $I_{Cl1-T}$  are due to the same channels (see below), we can estimate the relative subplasmalemmal Ca in response to release from stores and by SOCE by comparing the amplitude of  $I_{Cl1-S}$  immediately after  $IP_3$  injection with the amplitude of  $I_{Cl1-T}$  when SOCE is fully activated (Fig. 1, *A* and *B*). The fact that  $I_{Cl1-T}$  is usually twice as large as  $I_{Cl1-S}$  is consistent with the idea that subplasmalemmal Ca levels are lower in response to Ca release than they are to SOCE. The observations that injection of low concentrations of Ca into the oocyte or Ca influx through A-23187 channels selectively activates  $I_{Cl1-T}$  (Figs. 4 and 5) can be explained by these modes of Ca delivery being insufficient to provide enough Ca to activate  $I_{Cl2}$ .

The time course of activation of  $I_{Cl2}$  is considerably slower than that of  $I_{Cl1-T}$  (Fig. 3*C*). This can be explained if  $I_{Cl2}$  is less sensitive to Ca than  $I_{Cl1-T}$ . As SOCE develops,  $I_{Cl1-T}$  increases sooner than  $I_{Cl2}$ , simply because  $I_{Cl2}$  requires higher levels of Ca to be activated. The alternative explanation that  $I_{Cl2}$  activation requires intermediate steps between Ca influx and Cl channel activation is disfavored by the observation that Ca influx via heterologously expressed iGluR3 activates  $I_{Cl2}$  rapidly ( $<10$  s). Although this does not exclude the possibility that intermediates exist between Ca influx and Cl channel activation, this experiment shows that Ca influx can activate  $I_{Cl2}$  much more quickly than the activation that occurs in response to  $IP_3$  injection.

## How Many Types of Ca-Activated Cl Channels?

It is clear that *Xenopus* oocytes have several different Ca-activated Cl currents, which have different Ca sensitivities (4; present study), but whether these different currents are mediated by different channels remains to be established. These two currents could be due to two different Cl channels with different Ca affinities or one Cl channel with a Ca affinity that is dependent on voltage (Fig. 11). Any hypothesis needs to be able to explain the different waveforms of  $I_{Cl1-S}$ ,  $I_{Cl1-T}$ , and  $I_{Cl2}$  and also the differently shaped  $I-V$  relationships and ionic selectivities of these currents.

*Single-channel hypothesis.* The single-channel hypothesis suggests that  $I_{Cl1-S}$ ,  $I_{Cl1-T}$ , and  $I_{Cl2}$  are mediated by one Cl channel with voltage-dependent Ca affinity. The Ca affinity is greater at depolarized potentials. In response to  $IP_3$  injection,  $I_{Cl1-S}$  is stimulated as Ca is released from internal stores. The time-dependent activation of the current in response to a depolarizing voltage step could be attributed to a true voltage-dependent gating of the channel or a voltage-dependent increase in channel Ca affinity. The fact that the time-dependent component of the current disappears when large amounts of Ca are injected (Fig. 5*C*) is consistent with the idea that the voltage-dependent activation is due to an increase in Ca affinity. When Ca concentration is saturating, the time dependence is

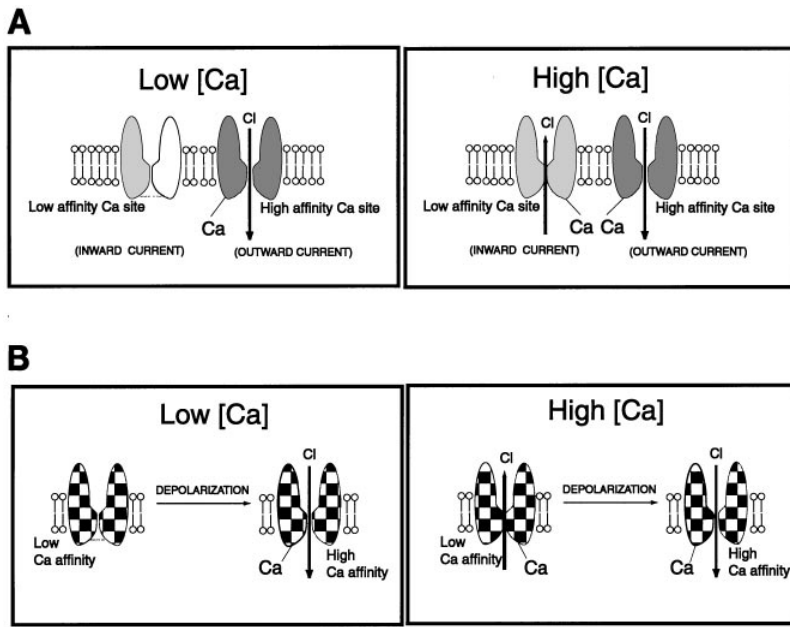


Fig. 11. Possible hypotheses to explain multiple Cl currents in oocytes. *A*: 2 different Cl channels with different Ca affinity. *B*: 1 Cl channel with voltage-dependent Ca affinity. [Ca], Ca concentration.

absent, because the channel is already maximally occupied with Ca. The deactivating tail current on hyperpolarization could be explained by a decrease in Ca affinity and/or voltage-dependent gating. The fact that one sees a large tail current even when large concentrations of Ca are injected to give a time-independent outward current is consistent with a change in Ca affinity. After Ca has been released from stores,  $I_{Cl1-S}$  turns off as the stores become depleted of Ca.  $I_{Cl2}$  is not activated in response to Ca release from stores, because at negative potentials the affinity of the channel for Ca is low and the subplasmalemmal Ca concentration in response to Ca release from stores is relatively low. After SOCE becomes activated in response to store depletion, Ca influx at hyperpolarized potentials activates  $I_{Cl2}$ . The time course of  $I_{Cl2}$  activation on stepping to  $-140$  mV is most likely explained by the time course of subplasmalemmal Ca accumulation during the pulse, because similar  $I_{Cl2}$  waveforms are seen with Ca influx through SOCs and through iGluR3. Repolarization to positive potentials evokes  $I_{Cl1-T}$  as a result of the voltage-dependent increase in Ca affinity of the channel. The different time course of stimulation of  $I_{Cl2}$  and  $I_{Cl1-T}$  after an  $IP_3$  injection can be explained simply by the lower Ca affinity of the channel at hyperpolarized potentials.

The single-channel hypothesis is reasonably successful in describing the waveforms of the currents in response to  $IP_3$  and Ca injection. However, can this hypothesis explain the difference in instantaneous  $I-V$  relationships (15) or the difference in anionic selectivities (Table 1) between the currents? Voltage-clamp data from the large oocyte can be problematic (see discussion in Ref. 52). In the case of the instantaneous  $I-V$  relationships, the large capacitance of the oocyte limited our ability to measure the tail currents  $<5$  ms after the voltage step. In fact, we usually measured the tails at 8 ms. Thus the instantaneous  $I-V$  relationships were

not truly instantaneous. If there are significant time-dependent currents that develop or decay during this time window, the instantaneous  $I-V$  relationships could be in error. For example, the instantaneous  $I-V$  relationship of  $I_{Cl2}$ , which is measured by depolarizing from  $-140$  mV (Fig. 9, *D-F*), would outwardly rectify if the Ca occupancy of the channel increased substantially during the 8-ms capacitive transient on depolarization as a result of an increase in Ca binding affinity. In contrast, the  $I-V$  relationship of  $I_{Cl1-S}$  or  $I_{Cl1-T}$ , which is measured by hyperpolarizing from a positive potential, could be more linear if the Ca occupancy changed more slowly on hyperpolarization. However, the tail currents on hyperpolarization are slower ( $\tau = 33$  ms on hyperpolarization from  $+80$  to  $-100$  mV) than the activation on depolarization ( $\tau = 14.5$  ms on depolarization to  $+40$  from  $-140$  mV).

The differences in anionic selectivities among the three currents are marginal with one exception: the difference in  $P_I/P_{Cl}$  between  $I_{Cl1-S}$  and the other two currents. For all other combinations, the differences in reversal potentials are  $<5$  mV, and the differences in calculated permeability ratios are not convincingly different. The difference in  $P_I/P_{Cl}$  between  $I_{Cl1-S}$  and the other two currents, however, represents an  $\sim 15$ -mV shift in reversal potential. Liquid junction potentials were carefully measured and were negligible, so it is difficult to see that this difference is due to a systematic error. The only way we can think to explain this difference, except by assuming two different Cl channels, is that the intracellular Cl concentration changes during the experiment.  $I_{Cl1-S}$  is measured within several minutes after impalement, whereas  $I_{Cl1-T}$  and  $I_{Cl2}$  are measured at least 10 min later.

The idea that Ca-activated Cl channels may exhibit voltage-dependent Ca binding has been proposed by Arreola et al. (1) for Ca-activated Cl channels in rat parotid acinar cells. These investigators show that the

Ca affinity of the channels increases as the membrane potential is made more positive. The apparent dissociation constant decreases from ~400 nM at -100 mV to ~60 nM at +100 mV. This is accompanied by an increase in the Hill coefficient from 1.2 to 2.4. It appears that the Ca-activated Cl channels in *Xenopus* oocytes may exhibit properties very similar to those of the channels in rat parotid.

**Multiple-channel hypothesis.** Much of the data we have presented can also be explained by assuming that there are several Cl channels with different Ca affinities. Outward currents are mediated by channels with high affinity, and inward currents are mediated by channels with low affinity. The multiple-channel hypothesis has the advantage that it can more easily explain the differences in the instantaneous *I-V* relationships and the ionic selectivities of the currents. However, one problem with the hypothesis that there are just two channels is that the ionic selectivity data suggest that  $I_{Cl1-T}$  and  $I_{Cl2}$  could be the same current, whereas the instantaneous *I-V* relationships suggest that they are not. Thus, if more than one channel is involved in mediating these currents, it seems that one must propose that there are three different kinds of channels.

#### Ca-Induced Ca Release

The idea that there is only one type of Cl channel would agree with the views of Parker and co-workers (30, 32, 35, 36, 49, 50) and Gomez-Hernandez et al. (13). However, we do not agree with the suggestion of Parker and co-workers that  $I_{Cl1-T}$  is due to Ca-induced Ca release. Parker has shown that, after release of Ca from stores stimulated by injection of  $IP_3$  into *Xenopus* oocytes, cytosolic Ca continues to increase after a hyperpolarizing voltage step has been terminated, presumably as a result of Ca-induced Ca release. He suggests that the outward current we call  $I_{Cl1-T}$  is actually  $I_{Cl2}$  being reactivated by Ca-induced Ca release. However, we find that heparin does not diminish the size of  $I_{Cl1-T}$  or  $I_{Cl2}$ , as would be expected if Ca-induced Ca release were contributing to the cytosolic Ca under these conditions. Also we do not observe continued increase in cytosolic Ca after terminating the hyperpolarizing step (24a). We believe that the difference between the results of Parker and co-workers and our results is the quantity of  $IP_3$  that was injected. Parker and co-workers injected a much smaller amount of  $IP_3$ , which resulted in Ca waves that were influenced by Ca influx. In contrast, we injected large amounts of  $IP_3$ , which rapidly depleted the stores completely so that there is little effect of Ca influx on release. Thus, although we agree with Parker and co-workers that the multiple currents may be explained by a single conductance, we believe that the currents are explained by a voltage-dependent change in Ca affinity, whereas Parker and co-workers believe that the different currents are explained by differences in Ca dynamics. Resolution of these questions will require single-channel analysis.

#### Physiological Significance of Cl Channels in *Xenopus* Oocytes

In the oocytes of many species, including *Xenopus*, sperm entry stimulates phosphatidylinositol 4,5-bisphosphate hydrolysis, production of  $IP_3$  (28, 43, 45), and release of Ca from internal stores. As the Ca wave spreads from the sperm entry site to encompass the entire egg, it activates Ca-activated Cl channels (15, 22), which depolarize the membrane to produce the fertilization potential (20, 47). Because amphibian eggs in the wild are fertilized in fresh water with relatively low Cl concentration,  $E_{Cl}$  is positive, and activation of Cl currents will depolarize the egg. The fertilization potential is responsible for the rapidly developing, transient block to polyspermy ("fast electrical block") (8, 14), which lasts ~15 min. The electrical block to polyspermy, which is found in many (but not all) species, is caused by a voltage dependence of sperm-egg fusion, with positive membrane potentials being inhibitory. This has been demonstrated by voltage-clamp experiments and by altering extracellular ionic composition to alter the polarity of the fertilization potential (9, 19, 27, 47). To prevent polyspermy, it is important that the depolarization develop rapidly. The voltage-dependent Ca sensitivity of Cl currents would provide a strong positive-feedback mechanism to accelerate the depolarization. Inasmuch as the egg depolarizes as the result of activation of Ca-activated Cl channels, the depolarization will increase the affinity of the channels for Ca, which will increase the depolarization. This feedback might be important in facilitating the rate of depolarization to block polyspermy.

We thank Alyson Ellingson and Elizabeth Lytle for excellent technical assistance, Dr. Khaled Machaca for comments on the manuscript, Dr. Jim Boulter for the iGluR3 plasmid, Dr. Raymond Dingledine for the iGluR3 cRNA, and Dr. Seiko Kawano for helpful discussion and for performing the experiment shown in Fig. 6 while she was visiting the author's laboratory.

This study was supported by National Institutes of Health Grants HL-21195 and GM-55276.

Address for reprint requests: H. C. Hartzell, Dept. of Cell Biology, 1648 Pierce Dr., Emory University School of Medicine, Atlanta, GA 30322-3030. E-mail: criss@cellbio.emory.edu.

Received 15 May 1998; accepted in final form 6 October 1998.

#### REFERENCES

1. **Arreola, J., J. E. Melvin, and T. Begenisich.** Activation of calcium-dependent chloride channels in rat parotid acinar cells. *J. Gen. Physiol.* 108: 35-47, 1996.
2. **Berridge, M. J.** Inositol triphosphate-induced membrane potential oscillations in *Xenopus* oocytes. *J. Physiol. (Lond.)* 403: 589-599, 1988.
3. **Berridge, M. J.** Elementary and global aspects of calcium signaling. *J. Physiol. (Lond.)* 499: 291-306, 1997.
4. **Boton, R., N. Dascal, B. Gillo, and Y. Lass.** Two calcium-activated chloride conductances in *Xenopus laevis* oocytes permeabilized with the ionophore A23187. *J. Physiol. (Lond.)* 408: 511-534, 1989.
5. **Boulter, J., M. Hollmann, A. O'Shea-Greenfield, M. Hartley, E. Deneris, C. Maron, and S. Heinemann.** Molecular cloning and functional expression of glutamate receptor subunit genes. *Science* 249: 1033-1037, 1990.
6. **Busa, W. B., and R. Nuccitelli.** An elevated free cytosolic  $Ca^{2+}$  wave follows fertilization in eggs of the frog, *Xenopus laevis*. *J. Cell Biol.* 100: 1325-1329, 1985.

7. **Camacho, P., and J. D. Lechleiter.** Calreticulin inhibits intracellular  $Ca^{2+}$  waves. *Cell* 82: 765–771, 1995.
8. **Cross, N. L., and R. P. Elinson.** A fast block to polyspermy in frogs mediated by changes in the membrane potential. *Dev. Biol.* 75: 187–198, 1980.
9. **Cross, N. L., and L. A. Jaffe.** Electrical properties of vertebrate oocyte membranes. *Biol. Reprod.* 30: 50–54, 1983.
10. **Dascal, N.** The use of *Xenopus* oocytes for the study of ion channels. *CRC Crit. Rev. Biochem.* 22: 317–387, 1987.
11. **Gillo, B., Y. Lass, E. Nadler, and Y. Oron.** The involvement of inositol 1,4,5-triphosphate and calcium in the two-component response to acetylcholine in *Xenopus* oocytes. *J. Physiol. (Lond.)* 392: 349–361, 1987.
12. **Gilon, P., G. St. J. Bird, X. Bian, J. L. Yakel, and J. W. Putney.** The Ca mobilizing actions of Jurkat extracts on mammalian cells and *Xenopus laevis* oocytes. *J. Biol. Chem.* 270: 8050–8055, 1995.
13. **Gomez-Hernandez, J.-M., W. Stuhmer, and A. B. Parekh.** Calcium dependence and distribution of calcium-activated chloride channels in *Xenopus* oocytes. *J. Physiol. (Lond.)* 502: 569–574, 1997.
14. **Grey, R. D., M. J. Bastiani, D. J. Webb, and E. R. Schertel.** An electrical block is required to prevent polyspermy in eggs fertilized by natural mating of *Xenopus laevis*. *Dev. Biol.* 89: 475–484, 1998.
15. **Hartzell, H. C.** Activation of different Cl currents in *Xenopus* oocytes by Ca liberated from stores and by capacitative Ca influx. *J. Gen. Physiol.* 108: 157–175, 1996.
16. **Hartzell, H. C., K. Machaca, and Y. Hirayama.** Effects of adenophostin-A and inositol-1,4,5-triphosphate on  $Cl^-$  currents in *Xenopus laevis* oocytes. *Mol. Pharmacol.* 51: 683–692, 1996.
17. **Hille, B.** *Ion Channels of Excitable Membranes.* Sunderland, MA: Sinauer, 1992.
18. **Hoth, M., and R. Penner.** Calcium release-activated calcium current in rat mast cells. *J. Physiol. (Lond.)* 465: 359–386, 1993.
19. **Jaffe, L. A.** Fast block to polyspermy in sea urchin eggs is electrically mediated. *Nature* 261, 68–71, 1976.
20. **Jaffe, L. A., and N. L. Cross.** Electrical regulation of sperm-egg fusion. *Annu. Rev. Physiol.* 48: 191–200, 1986.
21. **Kim, H. Y., D. Thomas, and M. R. Hanley.** Stimulation of  $Ca^{2+}$ -dependent membrane currents in *Xenopus* oocytes by microinjection of pyrimidine nucleotide-glucose conjugates. *Mol. Pharmacol.* 49: 360–364, 1996.
22. **Kline, D.** Calcium-dependent events at fertilization of the frog egg: injection of a calcium buffer blocks ion channel opening, exocytosis, and formation of pronuclei. *Dev. Biol.* 126: 346–361, 1988.
23. **Lechleiter, J. D., and D. E. Clapham.** Molecular mechanisms of intracellular calcium excitability in *X. laevis* oocytes. *Cell* 69: 283–294, 1996.
24. **Machaca, K., and H. C. Hartzell.** Asymmetrical distribution of Ca-activated Cl channels in *Xenopus* oocytes. *Biophys. J.* 74: 1286–1295, 1998.
- 24a. **Machaca, K., and H. C. Hartzell.** Reversible Ca gradients between the subplasmalemma and cytosol differentially activate Ca-dependent Cl currents. *J. Gen. Physiol.* In press.
25. **Miledi, R., and I. Parker.** Chloride current induced by injection of calcium into *Xenopus* oocytes. *J. Physiol. (Lond.)* 357: 173–183, 1984.
26. **Morgan, A. J., and R. Jacob.** Ionomycin enhances  $Ca^{2+}$  influx by stimulating store-regulated cation entry and not by a direct action at the plasma membrane. *Biochem. J.* 300: 665–672, 1994.
27. **Neher, E.** Correction for liquid junction potentials in patch clamp experiments. *Methods Enzymol.* 207: 123–131, 1992.
28. **Nuccitelli, R., D. L. Yim, and T. Smart.** The sperm-induced  $Ca^{2+}$  wave following fertilization of the *Xenopus* egg requires the production of  $Ins(1,4,5)P_3$ . *Dev. Biol.* 158: 200–212, 1993.
29. **Parker, I., J. Choi, and Y. Yao.** Elementary events of  $InsP_3$ -induced  $Ca^{2+}$  liberation in *Xenopus* oocytes: hot spots, puffs and blips. *Cell Calcium* 20: 105–121, 1996.
30. **Parker, I., C. B. Gundersen, and R. Miledi.** A transient inward current elicited by hyperpolarization during serotonin activation in *Xenopus* oocytes. *Proc. R. Soc. Lond. B Biol. Sci.* 223: 279–292, 1985.
31. **Parker, I., and I. Ivorra.** Inositol tetrakisphosphate liberates stored  $Ca^{2+}$  in *Xenopus* oocytes and facilitates responses to inositol trisphosphates. *J. Physiol. (Lond.)* 433: 207–227, 1991.
32. **Parker, I., and I. Ivorra.** Characteristics of membrane currents evoked by photoreleased inositol trisphosphate in *Xenopus* oocytes. *Am. J. Physiol.* 263 (Cell Physiol. 32): C154–C165, 1992.
33. **Parker, I., and I. Ivorra.** Confocal microfluorimetry of  $Ca^{2+}$  signals evoked in *Xenopus* oocytes by photoreleased inositol trisphosphate. *J. Physiol. (Lond.)* 461: 133–165, 1993.
34. **Parker, I., and R. Miledi.** Injection of inositol 1,3,4,5-tetrakisphosphate into *Xenopus* oocytes generates a chloride current dependent upon intracellular calcium. *Proc. R. Soc. Lond. B Biol. Sci.* 232: 59–70, 1987.
35. **Parker, I., and R. Miledi.** Inositol trisphosphate activates a voltage-dependent calcium influx in *Xenopus* oocytes. *Proc. R. Soc. Lond. B Biol. Sci.* 231: 27–36, 1987.
36. **Parker, I., and Y. Yao.** Relation between intracellular  $Ca^{2+}$  signals and  $Ca^{2+}$ -activated  $Cl^-$  current in *Xenopus* oocytes. *Cell Calcium* 15: 276–288, 1994.
37. **Petersen, C. C. H., and M. J. Berridge.** G-protein regulation of capacitative calcium entry may be mediated by protein kinases A and C in *Xenopus* oocytes. *Biochem. J.* 307: 663–668, 1995.
38. **Petersen, C. C. H., and M. J. Berridge.** Capacitative calcium entry is colocalised with calcium release in *Xenopus* oocytes: evidence against a highly diffusible calcium influx factor. *Pflügers Arch.* 431: 286–292, 1996.
39. **Petersen, C. C. H., M. J. Berridge, M. F. Borgese, and D. L. Bennett.** Putative capacitative calcium entry channels: expression of *Drosophila* trp and evidence for the existence of vertebrate homologues. *Biochem. J.* 311: 41–44, 1995.
40. **Pozzan, T., R. Rizzuto, P. Volpe, and J. Meldolesi.** Molecular and cellular physiology of intracellular stores. *Physiol. Rev.* 74: 595–636, 1994.
41. **Putney, J. W., Jr.** Inositol phosphates and calcium entry. *Adv. Second Messenger Phosphoprotein Res.* 26: 143–160, 1992.
42. **Putney, J. W., Jr.** Capacitative calcium entry revisited. *Cell Calcium* 11: 611–624, 1990.
43. **Snow, P., D. L. Yim, J. D. Leibow, S. Saini, and R. Nuccitelli.** Fertilization stimulates an increase in inositol trisphosphate and inositol lipid levels in *Xenopus* eggs. *Dev. Biol.* 180: 108–118, 1996.
44. **Snyder, P. M., K. Krause, and M. J. Welsh.** Inositol triphosphate isomers, but not inositol 1,3,4,5-tetrakisphosphate, induce calcium influx in *Xenopus laevis* oocytes. *J. Biol. Chem.* 263: 11048–11051, 1988.
45. **Stith, B. J., M. Goalstone, S. Silva, and C. Jaynes.** Inositol 1,4,5-trisphosphate mass changes from fertilization through first cleavage in *Xenopus laevis*. *Mol. Biol. Cell* 4: 435–443, 1993.
46. **Takahashi, T., E. Neher, and B. Sakmann.** Rat brain serotonin receptors in *Xenopus* oocytes are coupled by intracellular calcium to endogenous channels. *Proc. Natl. Acad. Sci. USA* 84: 5063–5067, 1987.
47. **Webb, D. J., and R. Nuccitelli.** Fertilization potential and electrical properties of the *Xenopus laevis* egg. *Dev. Biol.* 107: 395–406, 1985.
48. **Yao, Y., and I. Parker.** Potentiation of inositol trisphosphate-induced  $Ca^{2+}$  mobilization in *Xenopus* oocytes by cytosolic  $Ca^{2+}$ . *J. Physiol. (Lond.)* 458: 319–338, 1992.
49. **Yao, Y., and I. Parker.** Inositol trisphosphate-mediated  $Ca^{2+}$  influx into *Xenopus* oocytes triggers  $Ca^{2+}$  liberation from intracellular stores. *J. Physiol. (Lond.)* 468: 275–296, 1993.
50. **Yao, Y., and I. Parker.**  $Ca^{2+}$  influx modulation of temporal and spatial patterns of inositol trisphosphate-mediated  $Ca^{2+}$  liberation in *Xenopus* oocytes. *J. Physiol. (Lond.)* 476: 17–28, 1994.
51. **Yoshida, S., and S. Plant.** Mechanism of release of  $Ca^{2+}$  from intracellular stores in response to ionomycin in oocytes of the frog *Xenopus laevis*. *J. Physiol. (Lond.)* 458: 307–318, 1992.
52. **Zhang, Y., and D. McBride.** The ion selectivity of a membrane conductance inactivated by extracellular calcium in *Xenopus* oocytes. *J. Physiol. (Lond.)* 508: 763–776, 1998.
53. **Zweifach, A., and R. Lewis.** Rapid inactivation of depletion-activated calcium current ( $I_{CRAC}$ ) due to local calcium feedback. *J. Gen. Physiol.* 105: 209–226, 1995.